Simulation of Impact Regimes

Paul.W.Bland[1] * and Sarin Tiranasawasdi[1]

[1] Department of Mechanical Engineering Simulation & Design,
The Sirindhorn International Thai-German Graduate School of Engineering,
King Mongkut's University of Technology North Bangkok,
1518 Pracharaj 1 Road, Bangsue, Bangkok 10800, Thailand.

*Corresponding Author: Email: bland.p.mesd@tggs-bangkok.org (bland [dot] p [dot] mesd [at] tggs [dash] bangkok [dot] org)
Telephone Number: +66 (0) 2913 2500 ext. 2915, Fax. Number: +66 (0) 2913 2500 ext. 2922

Abstract

Impact regimes defined by projectile mass and velocity can produce very different characteristic target structural responses, and complex behaviour when the regime boundaries are crossed. This has previously been proven by experimental work. The objective of this work was to qualitatively model the experimentally observed impact behaviour, and to identify any deviation in trends between experiments and the simulation in terms of the type of response, but not in terms of material damage.

An explicit FE commercial package was used to simulate the impact of a free flying projectile onto a flat aluminium plate, varying projectile mass and velocity, target span and thickness. Behaviour was characterized by prediction of projectile-target contact time, projectile rebound velocity and target maximum deflection at its mid-span. Two extreme conditions of low velocity/high mass and high velocity/low mass were simulated, and the transition between these two regimes was explored by incrementally varying mass and velocity.

For low velocity/high mass, the simulation matched the main trends from the experimental work, with a classic quasi-static large scale global deflection type behaviour of sub first mode rebound. For high velocity/low mass, the agreement was less strong due to a lack of damage mechanics, but still confirming the response was localized to the contact zone. For the transitions between regimes, the simulation also matched the experimental work showing projectile-target intermittent contact when sweeping across the mass boundary, and a delay in global response when sweeping across the velocity boundary. Unlike the experimental work, the simulation allows the easy viewing of stress waves developing over time, that can be used to confirm and explain some of these observations.

Key words: Impact, regimes, boundaries, transition, simulation

1. Introduction

The study of impact problems is relevant to various engineering applications. There has been a significant amount of experimental research in a wide range of impact problems during the past two decades. Corbett et al. [1]

reviewed research into impact loading of plates by free-flying projectiles. Their comprehensive review covered 195 papers that included experimental studies, analytical modelling and code development in order to describe the characteristics of the penetration and perforation process for predicting the response of an impact loaded structure.

Impact behaviour has often been studied by using impact energy as one of the main control variables, realized physically by changing impact mass and/or velocity. Other key variables have been the projectile and or target material selection, properties and dimensions, clamping conditions and also angle of impact. Impact regimes have been defined by projectile mass and velocity [2-10], with theoretical boundaries separating impact regimes such as low-velocity impact and high-velocity impact, or low-velocity / high-mass (LV/HM) or high-velocity / low-mass (HV/LM). Generally, these regimes produce very different characteristic target structural responses when comparing the extremes. There has been less reported research studying the transition regions between any defined regimes or when the regime boundaries are crossed. It has been found that the projectile-structure interaction can be far more complex, when an impact occurs at or near such a boundary and brings into question the common definitions and terminology of impact regimes [7-12].

There has been extensive use of simulation techniques for impact problems, and a brief survey of work from 2008 to 2010 from selected journals suggests that a significant amount of work deals with new applications or the application of impact mechanics problem solving techniques to new problems, or new materials, or the continuation of studies for known problems with existing materials, especially composites. Examples are referenced here [13-16]. However, the authors could not find any reported literature specifically on the topic of simulating the transitions between impact regimes, or the underlying impact mechanics that explains the changes in observed behaviour as regimes are crossed.

Therefore, the purpose of this work was to begin to study previously experimentally observed transitions using simulation methods, and to identify any qualitative deviation in trends between experiments and the simulation in terms of the type of response.

The author's previous experimental work and subsequent related theoretical development [7-10] was used as the basis of comparison. The experimental work was applied to a modern carbon-fibre reinforced polymer, reporting the observations from two extreme impact conditions LV/HM defined by HV/LM, and the transition between both extreme conditions by varying projectile mass and velocity incrementally to sweep across the boundaries. The LV/HM impact condition can be described as Quasi-Static (QS) with relatively long contact times being sub first harmonic half period, without losing contact from first to last contact at the point of rebound, and large global deflection defined as being somewhere between the 1st mode profile and the profile of a static loading response. This can be easily modelled by a first approximation of a simple 1 DOF spring mass system. In contrast, for HV/LM, the contact duration was much shorter with highly localized

behaviour and no global deflection. For impact transition conditions, when sweeping across the boundaries by incrementally adjusting the impact velocity, there was an observed variation in the delay between first contact and significant formation of a global deflection. When sweeping across the boundaries by incrementally adjusting the projectile mass, there was an observed gradual introduction of a bouncing effect between the projectile and specimen, eventually leading to a loss of contact or discontinuous contact.

In order to simplify the first stage of simulation, it was decided not to model the same material, but to model an aluminium plate. This would remove material complexity, reduce simulation time, and avoid the damage mechanics generated within composites even for relative low impact energies. The focus was on the impact mechanics, looking at the target response, and not the damage mechanics, checking the qualitative behaviour and not the quantitative behaviour.

2. Finite element analysis approach

This section gives finite element modelling information for all impact cases. The modelling aimed to be representative of the qualitative simulation of the impact of a free flying projectile onto a flat aluminium plate. Both projectile and the plate were meshed with eight node solid elements, elastic-plastic strain hardening material model for the target and rigid material model for the projectile. The material properties for the aluminium target were density of 2.77E3 Kg/m^2, Young's Modulus of 71 *GPa*, Poisson's ratio of 0.33, yield strength of 280 *MPa*, and tangent modulus of 500 *MPa*. The material properties for the steel projectile were density of 7.85E3 Kg/m^2, Young's Modulus of 200 *GPa*, Poisson's ratio of 0.3, yield strength and tangent modulus not applicable.

The target dimensions were thicknesses of 2 and 6 *mm*, width of 80 *mm*, and spans of 100, 150, and 200 *mm*. For all targets, the two 80 *mm* wide edges were rigidly clamped, with the clamping surfaces themselves being 80 *mm* by 12.7 *mm.*

A 0.264 *g* steel sphere of diameter 4 *mm* was used for the LV/HM impact condition and a 3 *kg* mass with a hemispherical nose contact diameter of 12.7 *mm* was used for the HV/LM impact condition. Impact energy was set at 6.3, 16.8, 22.9 and 31.2 *J*. The corresponding velocities were 215, 355, 415, and 485 *m/s* for HV and 2.0, 3.3, 3.9 and 4.6 *m/s* for LV. These figures were chosen to make sure the impact events were well within their respective extreme regimes. This gave 48 impact condition cases, with simulation number coding as shown in Table 1.

Table 1. Simulation test number and test conditions for LV/HM and HV/LM. Test condition figures in brackets refer to the specimen thickness and span, in *mm*.

Test No.	Test condition	Impact energy *J*
01-04	LV/HM (2,100)	6.3, 16.8, 22.9, 31.2
05-08	LV/HM (2,150)	6.3, 16.8, 22.9, 31.2
09-12	LV/HM (2,200)	6.3, 16.8, 22.9, 31.2
13-16	LV/HM (6,100)	6.3, 16.8, 22.9, 31.2
17-20	LV/HM (6,150)	6.3, 16.8, 22.9, 31.2
21-24	LV/HM (6,200)	6.3, 16.8, 22.9, 31.2
25-28	HV/LM (2,100)	6.3, 16.8, 22.9, 31.2
29-32	HV/LM (2,150)	6.3, 16.8, 22.9, 31.2
33-36	HV/LM (2,200)	6.3, 16.8, 22.9, 31.2
37-40	HV/LM (6,100)	6.3, 16.8, 22.9, 31.2
41-44	HV/LM (6,150)	6.3, 16.8, 22.9, 31.2
45-48	HV/LM (6,200)	6.3, 16.8, 22.9, 31.2

For the simulation of transitions, the targets had a thickness of 2 *mm* and span of 150 *mm*, impacted by varying mass using a hemispherical nose contact diameter of 12.7 *mm* with an incremental range of masses from 17-95 *g* and for the velocity sweep, using a range of 15-96 *m/s*. The clamping condition was the same as for the LV/HM and HV/LM simulations. The test condition parameters were initially fixed by guess work, and subsequently altered in order to try to capture the boundary transition. The mass sweep impact conditions are summarised in Table 2. The velocity sweep impact conditions are summarised in Table 3.

Table 2. Simulation test number and test conditions for the mass boundary sweep cases. Test condition numbers are mass in *g*, and in brackets refer to impact velocity in *m/s* and impact energy in *J*, respectively

Test No.	Test condition	Test No.	Test condition
49	17 (11, 1.0)	58	27 (34,15.6)
50	17 (14, 1.6)	59	37 (27,13.5)
51	17 (20, 3.4)	60	37 (29,15.6)
52	17 (22, 4.1)	61	37 (33,20.2)
53	17 (28, 6.6)	62	63 (20,12.6)
54	17 (40,13.6)	63	63 (21,13.9)
55	17 (42, 15.0)	64	95 (16,12.1)
56	27 (27, 9.8)	65	95 (18,15.4)
57	27 (31,13.0)		

Table 3. Simulation test number and test conditions for the velocity boundary sweep cases. Test condition numbers are mass in *g*, and in brackets refer to impact velocity in *m/s* and impact energy in *J*, respectively

Test No.	Test condition	Test No.	Test condition
66	17 (56,26.7)	73	27 (69,64.3)
67	17 (61,31.6)	74	27 (96,124.4)
68	17 (72,44.1)	75	37 (37,25.3)
69	17 (95,76.7)	76	37 (45,37.5)
70	27 (15,3.0)	77	37 (53,52.0)
71	27 (50,33.7)	78	37 (63,73.4)
72	27 (53,37.9)	79	37 (88,143.3)

3. Results and discussion

All simulation cases were compared to previous experimental work, summarised below. None of the simulated targets were perforated due to not including damage mechanics, such as element deletion when stress levels reach some criterion. However, the yield stress was only just reached in test numbers 27,28,31,32,35,36,78, and 79 suggesting the driving impact mechanics would not have been seriously affected if damage mechanics were included. This may be sufficient for the qualitative study. The letter “P” in the graphs for experimental data indicate the targets were perforated.

3.1 Simulation results for the LV/HM regime

Overall, the LV/HM regime showed the closest agreement, matching the QS type behaviour observed in the experimental work.

3.1.1 Global deflection

Fig. 1 shows very good qualitative agreement between experiment and simulation, with deflection increasing for increasing impact energy for a given target, with deflection increasing with decreasing target stiffness for a given impact energy, and the gradients of those relationships increasing for decreasing specimen stiffness.

3.1.2 Residual projectile energy

Fig. 2 shows good qualitative agreement between experiment and simulation, when considering the effect of increasing impact energy or increasing span. All curves suggest non-linear relationships. The stiffest target from experimental work showed a maximum, which might suggest all curves would have maxima, but this is not proven. The effect of target thickness is less clear, as the experimental data

for 2 and 6 *mm* thick targets overlaps, but is separated for the simulation results. This may be a result from the effect of damage.

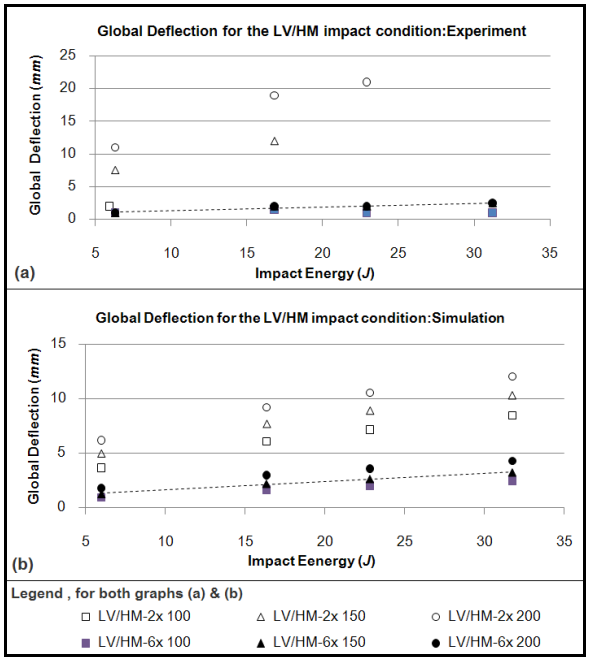

Figure 1. Global deflection for LV/HM experiment (a) and simulation (b).

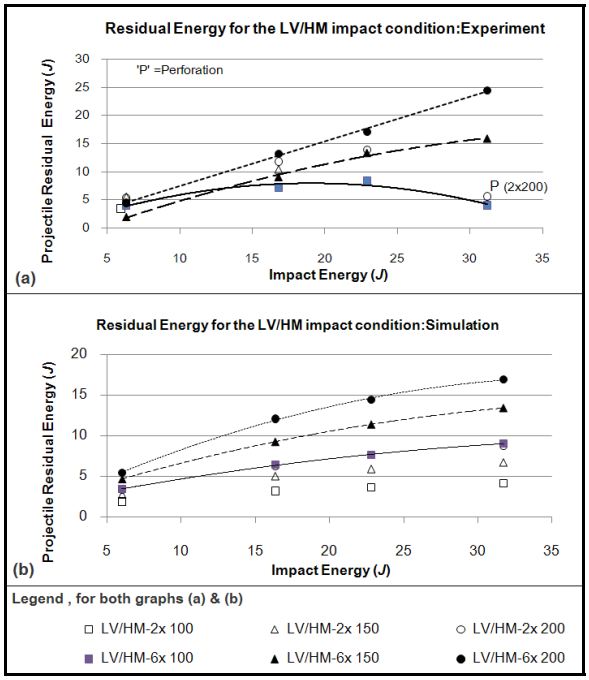

Figure 2. Projectile residual energy for LV/HM experiment (a) and simulation (b).

3.1.3 Contact duration

Fig. 3 shows good qualitative agreement between experiment and simulation, when considering the effect of target stiffness on contact duration, especially relating to 1st mode frequency and half period duration of lumped projectile-target being a good estimate of contact time. However, note that the simulation shows decreasing contact duration for increasing impact energy for the 2 *mm* thick targets.

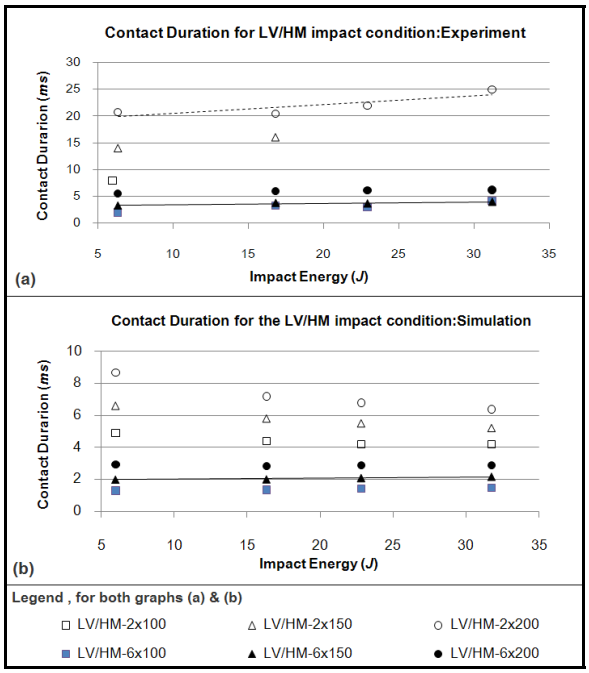

Figure 3. Contact duration for LV/HM experiment (a) and simulation (b).

3.2 Simulation results for the HV/LM regime

Overall, the HV/LM regime showed some agreement between simulation and experiment, but with key differences due to a lack of damage mechanics not allowing perforation. However, this reinforces the overall observation that the HV/LM response is a localised response, hence a high energy density in the response region.

Global deflection was zero or negligible for experiment and simulation, but with observable local deflection (localised directly at the contact point) for simulations. Local deflection could not be observed in experiments due to the high speed camera limitation. Fig. 4 shows residual projectile kinetic energy for all

simulations was between 0-0.6 *J*. For experiment, non-perforated conditions, it was 0.25-0.41 *J*. The quantitative comparison is not important, because of the different materials. The key point being, the values are much lower than the impact energy, and essentially viewed as constant within either the measurement errors or material damage mechanics modelling errors. Residual energy for experiments with perforation was much higher, due to the projectile continuing in flight once it had passed through the specimen. This is the key difference due to not having full damage mechanics modelling.

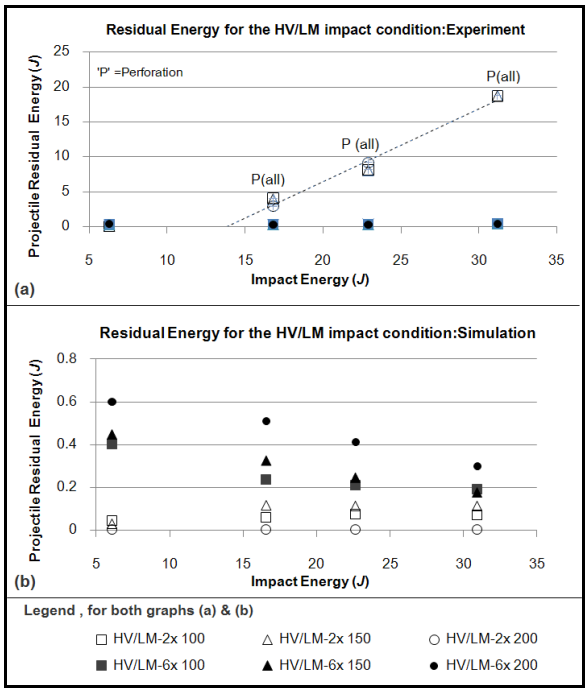

Figure 4. Projectile residual energy for HV/LM experiment (a) and simulation (b).

This problem is magnified for contact duration, which is even more dependent on local damage effects and hence little qualitative agreement. See Fig. 5.

3.3 Simulation results for the transitions

The experimental work defined criteria to identify the two transitions as intermittent contact "bounce" for the mass boundary, and delayed global deflection after first contact for the velocity boundary. The same criteria led to the following.

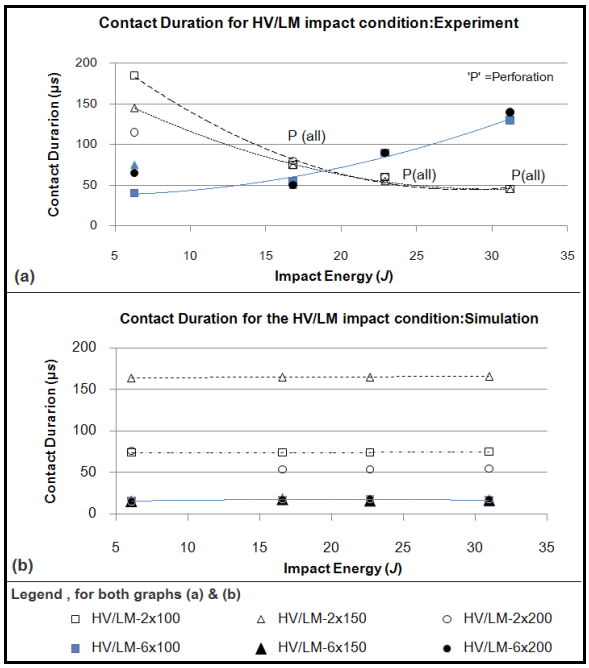

Figure 5. Contact duration for HV/LM experiment (a) and simulation (b).

3.3.1 Mass boundary sweep

Using the criteria of the boundary being defined by a change from continuous to discontinuous and then back to continuous contact, as the boundary is crossed, it was observed that the projectile masses of 17, 27 and 37 *g* resulted in discontinuous contact, and all other projectile masses above and below that resulted in continuous contact. Therefore, within the resolution of the chosen test parameters, the mass boundary covers the range of 17-37 *g*.

The velocities used for these tests were all in the LV range, except possibly for tests 54 and 55 where the velocities of 40 and 42 ms^{-1} were in the HV range.

3.3.2 Velocity boundary sweep

Although tests 66-79 were designed for the velocity sweep study, many of the tests from the mass boundary sweep study also proved useful in the velocity sweep study. For the 17,

27 and 37 *g* projectiles, the observed transitions occurred between 21-39, 27-31 and 27-29 ms^{-1} respectively. The ranges have some uncertainty due to not knowing if the transition would have been observed at slightly higher or lower velocities. The masses used were all in the mass boundary transition, but discontinuous contact occurred after the observation of delay or no delay was used for the velocity sweep criteria.

3.4 Stress wave propagation

For the extreme impact conditions, a simple but key difference is the notion of LV/HM being a global response and HV/LM being a localised response. As a starting point, this can be confirmed by observing the position of the stress wave first peak, referred to as the wave front. Normal stress was chosen to be observed, as this has been the standard in other literature [6].

For all LV/HM conditions, the wave front travelled and was reflected during the order of tens of microseconds, and continued such that bending stresses could be seen at the clamped boundary during the contact time lasting the order of milliseconds. For all HV/LM conditions, the wave front travelled and was reflected a maximum of two times, by the time contact was lost. The wave front had not even reached the clamped boundary for the 6 *mm* thick, 150 and 200 *mm* span targets. For the 6 *mm* thick, 100 *mm* span target, the wave had only just reached the boundary.

For the cases identified in sections 3.3.1 and 3.3.2 as being in the transitional boundaries, the stress wave results show a mixture of both the extreme LV/HM and the HV/LM stress wave results. This is referred to as mix mode, and confirms that the transition includes both types of behaviour.

Observing the development of the stress wave front can therefore give some insight into the experimental observations.

4. Conclusion

Previous experimental observations on impact extreme regimes of LV/HM and HV/LM, as well as regime boundary sweeps by varying velocity and mass incrementally, were confirmed by simulation. Key exceptions were for HV/LM, due to not including damage mechanics in the model. Observing stress wave front position during contact time also confirmed the key observations, and gives extra insight especially in showing mix mode behavior at the transitions.

Further work will also include increased resolution of incremental steps taken for projectile mass and velocity, and time steps used to view results; all requiring high computational time.

5. Acknowledgement

The presenter is grateful to the U.K. Institution of Mechanical Engineers for funding the attendance and formal representation of the IMechE at the conference.

6. References

[1] Corbett, G. G., Reid, S. R., Johnson, W. (1996). Impact Loading of Plates and Shells by Free-Flying Projectiles: A review, *International Journal of Impact Engineering*, Vol.18, 1996, pp.141-230.

[2] Olsson, R. (2000). Mass Criterion for Wave Controlled Impact Response of Composite Plates, *Composites Part A: Applied Science and Manufacturing*, Vol.31, 2000, pp.879-887.

[3] Olsson, R. (2001). Analytical Prediction of Large Mass Impact Damage in Composite Laminates, *Composites Part A: Applied Science and Manufacturing*, Vol.32, 2001, pp.1207-1215.

[4] Olsson, R. (2003). Closed Form Prediction of Peak Load and Delamination Onset under Small Mass Impact, *Composite Structures*, Vol.59, 2003, pp.341-349.

[5] Olsson, R., Donadon, M.V., Falzon, B.G. (2006). Delamination Threshold Load for Dynamic Impact on Plates, *International Journal of Solids and Structures*, Vol.43, 2006, pp.3124-3141.

[6] Malekzadeh ,K., . Khalili, M.R, Olsson, R., and Jafari, A. (2006). Higher-order Dynamic Response of Composite Sandwich Panels with Flexible Core under Simultaneous Low-Velocity Impacts of Multiple Small Masses, *International Journal of Solids and Structures*, Vol.43, 2006, pp.6667-6687.

[7] Bland, P.W. (2000). Impact Response and Performance of Carbon-Fibre Reinforced Polymers, PhD Thesis, Imperial College. University of London.

[8] Bland, P.W. and Dear, J.P. (2001). Observations on the Impact Behaviour of Carbon-Fiber Reinforced Polymers for the Qualitative Validation of Models, *Composites Part A: Applied Science and Manufacturing*, Vol.32, 2001, pp.1217-1227.

[9] Bland, P.W. and Pitakthapanaphong, S. (2005). Experimental Observations of Two Extreme Impact Conditions, paper presented in *The 19th Conference of Mechanical Engineering Network of Thailand*, October 2005, Phuket, Thailand.

[10] Bland, P.W. and Pitakthapanaphong, S. (2005). A Discussion on the Role Played by Velocity in Impact Mechanics, paper presented in *The 19th Conference of Mechanical Engineering Network of Thailand*, October 2005, Phuket, Thailand.

[11] Bland, P.W. and Chollacoop, N. (2006). Experimental Observations of Mass and Velocity Parametric Sweeps of Impact Regime Boundaries, paper presented in *The 20th Conference of Mechanical Engineering Network of Thailand*, October 2006, Nakhon Ratchasima, Thailand.

[12] Bland, P.W. and Chollacoop, N. (2006). On the Concept and Application of Impact Response Maps, poster presented in *The 20th Conference of Mechanical Engineering Network of Thailand*, October 2006, Nakhon Ratchasima, Thailand.

[13] Iqbal, M.A., Gupta, G., Gupta, N.K. (2010). 3D Numerical Simulations of Ductile Targets Subjected to Oblique Impact by sharp Nosed Projectiles, *International Journal of Solids and Structures*, Vol.47, 2010, pp.224-237.

[14] Tham, C.Y., Tan, V.B.C., Lee, H.P. (2008). Ballistic Impact of a KEVLAR Helmet: Experiment and Simulations, *International Journal of Impact Engineering*, Vol.35, 2008, pp.304-318.

[15] Chang, C.-L., Yang, S.-H. (2009). Simulation of Wheel Impact Test using Finite Element Method, *Engineering Failure and Analysis*, Vol.16, 2009, pp.1711-1719.

[16] Wicklein, M., Ryan, S., Whire, D.M., Clegg, R.A. (2008). Hypervelocity Impact on CFRP: Testing, Material Modelling and Numerical Simulation, *International Journal of Impact Engineering*, Vol.35, 2008, pp.1861-1869.